Analyst

Accepted Manuscript

ROYAL SOCIETY OF CHEMISTRY

www.rsc.org/analyst

A triple-amplification colorimetric assay for antibiotics based on magnetic aptamer-enzyme co-immobilized platinum nanoprobes and exonuclease-assisted target recycling

Yangbao Miao[a], Ning Gan*[,a], Hong-Xia Ren[c], Tianhua Li[a], Yuting Cao[a], Futao Hu[a], Zhongdan Yan[a],Yinji Chen[b]

[a] Faculty of material science and chemical engineering, Ningbo University, Ningbo, China, 315211

[b] Faculty of Food Science and Engineering, Nanjing University of Finance and Economics, Nanjing, China, 210000

[c] Key Laboratory of Asymmetric Synthesis and Chirotechnology of Sichuan Province, Chengdu Institute of Organic Chemistry, Chinese Academy of Sciences, Chengdu, China, 610041

Abstract:

Herein, an ultrasensitive and selective colorimetric assay for antibiotics, using chloraphenicol (CAP) as model analyte, was developed based on a magnetic aptamer-HRP-platinum composite probes and exonuclease-assisted target recycling. The composite probes were prepared through the immunoreactions between the double strand DNA antibody (anti DNA) labeled on core-shell Fe_3O_4@Au nanoparticles (AuMNPs-anti DNA) as capture probe, and the double strand aptamer (aptamer hybrid with its complementary oligonucleotides) labeled on Pt@HRP nanoparticles as nanotracer (ds-Apt-HRP-PtNPs). When the CAP samples were incubated with the probes for 30 min at room temperature, it can be captured by the aptamer to form the nanotracer-CAP complex, which was then released into the supernatant after magnetic separation. This is because anti DNA on capture probes can't recognize the single strand aptamer-CAP complex. The exonuclease I (Exo I) added into the supernatant can further digest the aptamer-CAP from the 3′-end of aptamer and the CAP in aptamer-CAP complex can be released again, which can further participate in new cycling to react with the probes. Pt and HRP in the nanotracer could both catalyze and dual amplify the absorbance at 650nm ascribed to 3,3',5,5'-tetramethylbenzidine (TMB)-H_2O_2 system. Moreover, the Exo I can assist the target recycling, which can further amplify the signal. Thus, the triple amplified signal can be quantified by ultraviolet-visible spectroscopy. Experimental results showed that the CAP detection owned a linear range of 0.001-10 ng mL^{-1} and detection limit of 0.0003 ng mL^{-1}(S/N=3). The assay was successfully employed to detect CAP in milk, which is much facile, time saving, sensitive than the commercial ELISA kits.

Keywords: colorimetric aptamer sensor, dsDNA antibody, magnetic enzymatic probes, chloraphenicol**,** Pt NPs@HRP

1. Introduction

Antibiotics are widely used for treating and preventing infectious diseases of poultry against gram-positive and gram-negative microorganisms [1-2]. However, the accumulation in human bodies from trace residue of the antibiotics in meat and milk can cause serious allergic reactions and general immunity lowering. So, the Maximum Residue Level (MRL) of chloramphenicol (CAP) of European Union in food is just 0.3 μg kg^{-1} [3-5]. Therefore, it is essential to develop a facile, speedy and sensitive screening method for antibiotics in food. Recently, many assays were used for antibiotics detection. For instances, the optical sensor [6], the chemiluminescent enzyme-linked immunosorbent assay (CL-ELISA) [7], the high-performance liquid chromatography–tandem mass spectrometry HPLC–MS/MS [8], the neutral desorption-extractive electrospray ionization mass spectrometry (ND-EESI-MS) [9], the liquid chromatography–tandem mass spectrometric (LC–MS/MS) [10], the quartz crystal microbalance (QCM) [11], the inductively coupled plasma mass spectrometry (ICP-MS) [12], the multiwalled carbon nanotubes@molecularly imprinted polymer [13]. All of them have been successfully applied in food control fields. However, these methods still remain some shortcomings. For example, expensive equipment is required, the sample preparation processes are complicated, and some of them are time-consuming and not suitable for on-site analysis. To overcome such above shortcomings, the colorimetric assay based on aptamer probes may be a better choice, which had aroused wide public concerns in the past two decades [14-16]. Aptamer is one kind of single-stranded oligonucleotide with fixed sequences, which has been considered as promising probes instead of protein antibody for selectively recognizing the analytes [17-19]. Aptamers not only have almost all the advantages of antibodies, but also unique merits, such as thermal stability, low cost, and easily being duplicated by polymerase chain reaction (PCR) [17-19, 20]. Generally, the principle of colorimetric aptamer sensor (aptasensor) is based on two aspects. One is to use the aptamer labeled on probe to capture the analyte; the other is that after the isolation of analyte, some signal tracer on the sensor, such as a enzyme, can be released and induce the color development [21,22].

First of all, it's important to fabricate a selective and effective capture probe to isolate the target. In our study, the capture probes were composed of double strand DNA antibody (anti DNA) labeled on Fe_3O_4@Au nanoparticles (AuMNPs @anti DNA). The reason of why we choose the double strand DNA antibody as ligand is because it can react with the hybrid double stand aptamer selectively by antigen-antibody binding [23]. Accordingly, Emlen, Ansari, and Burdick have demonstrated that a 35-45-base pair (bp) DNA fragment is protected from DNase digestion and can remain bound to antibody to form a small, DNase resistant DNA-anti DNA immune complex [23,24]. (ds-Apt, aptamer and its complementary oligonucleotides).

The secondary consideration for the fabrication of our assay is to choose a sensitive signal tracer to induce the color development [25]. HRP, as a kind of enzyme tracer, is used widely in colorimetric sensor for color transition, which can catalyze a variety of substrates such as 3,3',5,5'-tetramethylbenzidine (TMB) [26,27], to form colorful products at 650nm. Recently, the noble metal nanoparticle-enzyme co-immobilized nanotracer for aptasensor has a tremendous promise in realizing ultrasensitity and high selectivity for the detection of targets [28]. Pt and HRP both could efficiently catalyze TMB-H_2O_2 solution for dual amplifying the color development [29], which can be quantified by ultraviolet-visible spectroscopy. Thus, in this research, the double strand CAP aptamer (ds-Apt, aptamer hybrid with its complementary sequences) labeled on ds-Apt-HRP-PtNPs nanotracer (ds-Apt- ds-Apt-HRP-PtNPs) was synthesized and employed as nanotracer. The reason of why we chose ds-Apt as the recognition component on the nanotracer is because it can be easily connected with capture probe to form the composite probe based on an immunoreactions between ds-Apt and anti DNA. Moreover, after the composite probes reacting with CAP and magnetic separation, the nanotracer can be translated into the single strand of complementary Apt (cApt) and CAP-Apt-HRP-Pt complex, which both can't be recognized by anti DNA on capture probe and then be released into supernatant. HRP-Pt in the complex can then catalyze the TMB-H_2O_2 solution system to develop a blue color.

In order to further amplify the signal, Exonuclease I (Exo I), as a kind of processive single-strand DNA specific enzyme, was further employed for enhance the color absorbance. Exo I can digest single-strand DNA in the direction of 3′ to 5′ [30] and release CAP again for probe reaction. The exonuclease-assisted target recycling is very convenient which need no further immobilization step, and just need to inject the Exo I into the supernatant, thus it has been widely used for signal amplification [31].

Inspired by the such above advantages of the materials, our motivation in this work is to exploit a triple signal-amplified colorimetric assay for the detection of ultra-trace level of antibiotics (defined as 0.1 ppb, which can detect trace amounts of the following target) [32,33], using CAP as model, based on the magnetic aptamer-HRP-Pt NPs nanotracer and Exo I-assisted target recycling amplification. In the assay, the magnetic composite probes was firstly prepared by connecting the AuMNPs @anti DNA particles with ds-Apt-HRP-Pt nanotracer, which was composed of double strand DNA(aptamer hybrid with its complementary sequence) labeled on HRP-Pt composite. The detection procedure was shown in scheme 1. When CAP samples was captured by the aptamer on the probes and after magnetic separation, the CAP-nanotracer complex(CAP-Apt-HRP-Pt) and its complementary single strand (cApt) will be released into supernatant, because the aptamer and cApt can't be recognized by the double strand DNA antibody on capture probes. Then, Exo I in the supernatant solution can selectively digest the CAP-Apt-HRP-Pt from the 3′-end of aptamer and the CAP in aptamer-CAP complex can be released again for analyte recycling. The ds-Apt-HRP-PtNPs in the nanotracer can dual catalyze and amplify the color produced by TMB and H_2O_2. Moreover, the Exo I-assisted target recycling can further amplify the signal. In this way, the assay based on proposed aptamer provided a triple amplified signal, and achieved rapid, sensitive and selective detection of CAP. And the detection limit can be greatly decreased to 0.01ng/mL and observed by naked eyes. The preparation of biosensor is complicated. However, the whole preparing procedures of signal tag (ds-Apt-HRP-Pt) are based on self-assembly technique without using the covalent chemical reagents, e.g. EDC, NHS. Thus, it's relatively feasible for repentance of the experiments by commercial companies. Moreover, there

is only one step in the testing process. If changing the aptamer for targets besides chloramphenicol, it can also be used to detect other analytes with only one step. The assay was successfully employed to detect CAP in real milk samples and the results were compared with these by commercial ELISA.

Preferred position for Scheme.1

2. Regents and methods

2.1 reagents and chemicals

The oligonucleotides used in this paper are as the following sequences: thiolated 40 mer Apt [34], 5'$(CH_2)_6$-ACT TCA GTG AGT TGT CCC ACG GTC GGC GAG TCG GTG GTAG; thiolated 40- mer complementary DNA (cDNA), 5'SH-$(CH_2)_6$-CTA CCA CCG ACT CGC CGA CCG TGG GAC AAC TCA CTG AAGT were purchased from Shanghai Sangon Biological Engineering Co., Ltd (Shanghai, China). CAP, streptomyces erythreus (ME), oxytetracycline (OTC), chlortetracycline (CTC), kanamycin (Kana) and gentamicin sulfate (GS) were purchased from Sigma Co., Ltd (Milan, Italy). Hydrogen tetrachloroaurate(III) tetrahydrate $HAuCl_4$, Ferric chloride ($FeCl_3 \cdot 6H_2O$), sodium acetate anhydrous (NaAc), hydrogen peroxide (H_2O_2, 30%) and 3,3',5,5'-tetramethylbenzidine (TMB) were obtained from Sinopharm Chemical Reagent Co., Ltd (Shanghai, China). The ds-DNA antibody ELISA Kit, Exo I and its buffer were purchased from Takara Biotechnology Co. Ltd. (Dalian, China). Tris(2-carboxyethyl) phosphine hydrochloride (TCEP) were purchased from Sigma-Aldrich. All other reagents were analytical grade and were used without further purification. Double-distilled water was used throughout the study.

2.2 Preparation of AuMNPs

AuNPs colloide was prepared with the slight modified Frens method [35]. And its diameter is about 20 nm. Fe_3O_4 microsphere synthesis used a solvothermal reaction by Li's method [36]. AuMNPs were synthesized as described in the previously reported literature with minor modifications [37]. Above all, 0.02 g Fe_3O_4 nanospheres was dispersed in 5 mL 3 % PDDA aqueous solution and rapidly stirred for 30 min. After

magnetic separation and washed by 100 mL of 0.1 mol/L PBS buffer (pH 7.4) for several times, it was re-dispersed into solution. Next, 5mL purple 1mg/mL AuNPs solution was slowly dropped into the supernatant, and react for 4h by stirring. After that, the AuMNPs was synthesized by washing several times with deionized water and ethanol respectively. Subsequently, the solution was dispersed into 100 mL of 0.1 mol/L PBS buffer (pH 7.4). Before use, the solution was stockpiled at 4°C.

2.3 Synthetic of AuMNPs-anti DNA capture probes

The immobilization of CAP Apt onto Au MNPs was carried out according to the procedure as previously reported with some modification [38]. 1ml of Au MNPs and 4 μL of 0.01% (v/v) antibody of dsDNA was mixed in 0.1 mol/L PBS buffer (pH 7.4) , then incubated for 30 minutes. After magnetic separation, the precipitation was washed for 3 times by the PBS buffer and re-dispersed into supernatant for usage.

2.6 Preparation of the ds-Apt-Pt-HRP nanotracer and the composite probes

200 μL 1 μM thiol-Apt thiolated 40 mer Apt and its complementary strand（2 ODs）[39] was hybrid in the PBS solution at 42℃ for 30min. Taking 150μL 1mg/mL prepared PtNPs (diameter of 5nm) prepared by the method [40] then adjusting to pH 8.2 with sodium carbonate buffer, 150 μL 2 mg/ml of HRP was following added then reacted for 6 hours at 4℃. After 12000 r/min centrifugation for 10 minutes, the precipitate was repeatedly washed for three times with PBS buffer solution. Then obtained adsorbent was added to 200μL ds-Aptamer and incubated for 60 minutes at 37 ℃. The resulting conjugations were incubated in BSA solution (100 μL 3% (w/v) BSA) at room temperature for about 30 minutes so as to block possible active sites and prevent the non-specific absorption [41]. Soon afterwards, the nanotracer was distributed in 0.1 mol/L PBS buffer solutions (pH 7.4). Then the mixture is reserved in 4 ℃ before usage.

The composite probes were synthesized by adding 100 μL capture probe to 200 μL nanotracer. The mixture was stirred gently for 2 hours at 37 ℃, ultimately resulting in the magnetic probes. Then after magnetic separation, the precipitated composite

probes were re-dispersed in 200 μL 0.1 mol/L PBS buffer solutions (pH 7.4) and stored in 4℃.

2.4 The colorimetric development for CAP detection

The manufacturing procedure of the colorimetric aptasensor for CAP is demonstrated in Scheme.1. In order to detect CAP, 200 μL variable concentration of CAP containing 20 U Exo I was incubated with the probe for 30 min at room temperature. After incubation, the supernatant was obtained by a magnet separator. Subsequently, 0.85 μM TMB 0.45 μM H_2O_2 were added to the supernatant in order, the change of color can be observed by the naked eye. Finally, the solution was shaken plentifully for color development and the absorbance was determined at 650 nm by UV-vis spectrometer for quantitative analysis.

2.5 The detection of CAP in real milk samples

Several milk samples in supermarket was employed for testify the application of the proposed method. Firstly, 2.0 g milk sample was weight and then was placed in 50 ml centrifuge tube. Subsequent, 4 mL 3% (w/v) trichloroacetic acid aqueous solution was added, followed by a whirl until smooth and then addition of 2 ml methanol and a thoroughly shake. After centrifugation 10 min at 4000 r/min, 3ml the supernatant was dried at 50~ 60℃ under nitrogen atmosphere and then resolved in water for the detection by the developed aptasensor. We choose the extraction liquid in blank milk to testify the matrix interference in real samples. ELISA method was performed in Microplate Reader in 96-cell Plate according the protocol of kits.

3. Results and discussion

3.1 Characterization of AuMNPs and AuMNPs-anti DNA capture probes

AuMNPs and AuMNPs-anti DNA capture probes were characterized by scan electron microscope (SEM) and UV-vis spectrophotometer, and the results were shown in Fig. 1. Fig1A showed that the average diameter of spherical Fe_3O_4

nanospheres was 205 nm. From Fig1B, there were many AuNPs with diameter of about 20 nm adhering to the surfaces of Fe_3O_4 NPs, which confirmed that AuMNPs was successfully synthesized. It revealed that the Au MNPs has a mean hydrodynamic diameter of 242.25 nm by laser particle size analyzer (Figure S1; see Supporting Information). After AuMNPs were labeled with antibody, the surface of Au MNPs became smooth and with an obvious coating on it (Fig 1C). These proved that anti DNA maybe conjugated on the Au NPs of AuMNPs. The ultraviolet visible absorption spectra of Fe_3O_4NPs (Fig 1D-a), AuNPs (Fig 1D-b), dsDNA Ab (Fig 1D-c), AuMNPs (Fig 1D-d), AuMNPs-dsDNA Ab conjugates (Fig 1D-e), were also shown. As shown in Fig. 1D-a, bare Fe_3O_4 showed no absorption from 200 nm to 800 nm, and AuMNPs showed a maximum absorption peak at 538 nm(curve d) which can be ascribed as the red shift of the characteristic peak of bare AuNPs at 520 nm(curve b), which may be the interaction between AuNPs and Fe_3O_4 nanoparticles. From curve e, the absorption peak at 276 nm (the characteristic peak of antibody from curve c) and at 542 nm (red shift of AuNPs after reacting with antibody) were both observed on the UV-vis in AuMNPs@anti DNA (Fig 1D-e), indicating that the antibody was successfully bound onto Au MNPs to form the capture probes.

Preferred position for Fig. 1

3.2 Characterization of nanotracer and its components

PtNPs, ds-Apt-HRP-PtNPs, ds-Apt-HRP-PtNPs nanotracer were characterized by Transmission Electron Microscope (TEM) and UV-vis spectrophotometry. The results were shown in Fig. 2. The size of PtNPs was about 5 nm in diameter (Fig. 2A). Meanwhile, in Fig. 2B, there was some visible dark shadow around Pt nanoparticles (PtNPs), which means that HRP was coated on Pt NPs to form HRP-PtNPs particles. Fig. 2C showed the UV-vis absorption spectrum of ds-Apt DNA (Fig1C-a), PtNPs (Fig1C-b), ds-Apt-HRP-PtNPs (Fig1C-c) and ds-Apt-HRP-PtNPs nanotracer (Fig1C-d). The ds-Apt DNA showed characteristic peak at 260nm. The bare PtNPs exhibited no absorption peak (curve b). We could observe the absorption peak at 278

nm and 402 nm in ds-Apt-HRP-PtNPs (curve c), which was ascribed to HRP's characteristic absorption [42]. The ds-Apt-HRP-PtNPs illustrated two characteristic absorption peaks at 258 nm (DNA) and 405 nm (HRP). It can prove that the ds-Apt-HRP-PtNPs was successfully synthesized [42]. We also use energy-dispersive X-ray spectroscopy to characterize the ds-Apt-HRP-PtNPs nanotracer. The characteristic peak of Pt (2.01 keV) and phosphorus (2.035 keV, ascribed to aptamer) can be obviously seen. All these proved that the nanotracer was successfully synthesized.

Preferred position for Fig. 2

3.3 The detection mechanism and triple signal amplification performance

In order to verify this detection principle, some controlled experiments were performed. Fig.S2 showed the UV-vis spectrum of TMB solution under various conditions. It can be seen that, in the absence (curve a) and in the presence (curve b) of H_2O_2, TMB solution exhibited no characteristic peak in the range of 550 - 750 nm. Moreover, in the absence of ds-Apt-HRP-Pt nanotracer, the TMB-H_2O_2 mixture solution exhibited no characteristic peak. The TMB-H_2O_2 mixture solution exhibited a strong absorption peak at 650 nm after the ds-Apt-HRP-Pt nanotracer was added for about 5 min at room temperature, which should be attributed to the redox reaction of TMB-H_2O_2 caused by nanotracer.

In order to verify the triple signal amplification effect, the colorimetric response of the aptasensor in the absence and presence of PtNPs, HRP, ds-Apt-HRP-PtNPs nanotracer, Exo I were detected. As shown in Fig.3, when 1 μM CAP was added into TMB-H_2O_2 system, the response signal at 650nm increased to 0.054 (curve b and insert b) by using ds-Apt- PtNPs nanotracer and signal at 650nm increased to 0.090 (curve c and insert c) by using ds-Apt-HRP tracer compared with that no CAP was added (curve a and insert a). While using the ds-Apt-HRP-PtNPs nanotracer, the response increased to 0.242 (curve c and insert c). All these proved that both PtNPs

and HRP can both catalyze the color development in TMB-H_2O_2. Moreover, after 0.1mL 20 U Exo I was added into reaction system , the signal increased significantly to 3.524 (curve d) by 14.56 folds, which means that the Exo I-assisted target recycling leads more dissociation of nanotracer on the sensor platform released to the supernatant and amplifies the peak. It can be concluded that ds-Apt-HRP-PtNPs, Exo I has triple signal amplification effect to achieve high sensitivity for the target.

In order to demonstrate the feasibility of the signal amplification of Exo I, the Gel electrophoresis experiment was introduced. In the Figure S3 from lane 3, we can observe that in the absence of ExoI, only a bright band of aptamer from CAP-signal tag complex in supernatant could be observed. This proved that CAP can't be released from signal tag without the hydrolysis of ExoI and the assisted target recycling amplification was inhibited. However, when adding 20U ExoI into the supernatant containing CAP signal tag complex, there was no fluoresence bands, which could also be observed in lanes of 2 as blank, which indicated that the Exo I can successful hydrolyse ssDNA on signal tag and assist target recycling.

Preferred position for Fig. 3

3.4 Optimization of experimental condition

It is well-known that the colorimetric response was closely related to pH, reaction time between the probe and CAP, the amount of Exo I and incubation temperature. Results revealed that pH 7.4 was optimum (Fig 4A) and 30 min of incubation time was selected when the curve tendency reached to the plateau in Fig 4B. It could be seen from Fig4C that the absorbance value was changed when adding 0.1ml Exo I with the concentration of 0 to 25 U for target recycling, and the maximum absorbance value was obtained at 20 U (curve c). The incubation temperature from 25 ℃ to 40 ℃ was observed and the maximum absorbance value was obtained at 37 ℃.

Other conditions such as the optimal concentration of TMB, H_2O_2, ds-Apt-HRP-PtNPs and the amount of magnetic compostie probes were illustrated in Fig. S1. As demonstrated in Fig. S1 (A), with the increasing concentration of TMB,

the absorbance sharply increased and reached a steady value when a higher concentration (⩾0.85 μM) was used. Therefore, 0.85 μM was chosen as the most favorable TMB concentration. As shown in Fig. S1 (B), the value of absorbance increased with the addition of higher H_2O_2 concentration and leveled off to a saturation value at 0.45 μM of H_2O_2. As shown in Fig. S1 (C), the catalytic time of Pt NPs-HRP in the supernatant was in the range of 0 min to 18 min. Fig. S1 (D) showed the value of absorbance enhanced with the addition of increasing concentration of magnetic compostie probes, and the largest value was acquired at the concentration of 1mg mL^{-1} of probes .

Preferred position for Fig. 4

3.6 Selectivity and specificity of aptasensor

In order to further investigate the selectivity of the proposed colorimetric analysis, we applied five other antibiotics, including streptomyces erythreus (ME), oxytetracycline (OTC), chlortetracycline (CTC), kanamycin (Kana) and gentamicin sulfate (GS). Respectively, they were individually added into the TMB-H_2O_2 system with 0.85 μM TMB, 0.45 μM H_2O_2, and then detected by the aptasensor. As demonstrated in Fig. 5, the absorbance of the 10 ng mL^{-1} CAP alone was much higher (10 folds) than that of other antibiotics, which means the probes can only recognize CAP. In order to further demonstrate selectivity of the assay, the cross-reactivity of CAP and CAP mixture with other antibiotics were tested. In Fig. 5, it was clearly shown that there was nearly negligible signal changes compared with 10 ng mL^{-1} CAP when adding the mixture of 10 ng mL^{-1} CAP containing 10 ng mL^{-1} other antibiotics. Above-mentioned consequences indicated that there was no cross-reactivity for other antibiotics and the colorimetric aptasensor could be used to selectively determinate CAP.

Preferred position for Fig. 5

3.7 Analytical performance of the colorimetric aptasensor

Under the optimal conditions, the sensitivity and detection range of colorimetric assay were checked with a series of concentrations of CAP based on the absorbance at 650 nm. As shown in Fig.6, the absorbance increased linearly with the concentration of CAP varied from 0.001 ng ml^{-1} to 10 ng ml^{-1}. The relationship can be described as y=0.111ln(x)+0.884. The correlation coefficient is 0.997, demonstrating a favorable linear relationship. The detection limit was 0.0003 ng ml^{-1} （S/N=3). As shown in Fig. 6C, the color transform of various concentrations of target CAP (0, 0.01, 0.02, 0.05, 0.1, 0.2, 0.5, 1, 2, 5, 10 ng mL^{-1}, respectively) would be distinguished with naked eye. Such low detection limit could be ascribed to the triple signal amplification of ds-Apt-HRP-PtNPs nanotracer and ExoI-assisted target recycling. The reproducibility of the sensor system was appraised through five repeated measurement of 10 ng mL^{-1} of CAP and the relative standard deviation (RSD) was about 2.4 %. The results indicated that the proposed method can be employed for the detection of CAP with a wide range of concentration.

We also listed many recent literatures detecting CAP in Table 1. Among these cited papers, the lowest detection limit was 0.0054 ng mL^{-1} using electrochemical immunoassay method, and the corresponding linear range was between 1.6-1292.5 ng mL^{-1}. In our study, the detection limit was as low as 0.0003 ng mL^{-1} and the linear relational concentration range was as wide as 4 orders of magnitude. Moreover, our reaction time only needs 30 min, which showed that our method was the most rapid among the listed literatures.

Preferred position for Fig. 6

3.8 Analytical application

The feasibility of our method was evaluated with real milk samples with a certain amount of CAP from local supermarket. The obtained results were compared with those of the ELISA method in Table 2, which were almost identical without significant difference. The accuracy of CAP detection in fish samples were also

evaluated by determining the recovery of CAP by a standard addition method, into which a known quantity of CAP (0.10, 1.00 ng mL^{-1}, respectively) was added. As shown in Table 2, the recoveries were all between 90.0% and 100.8%, indicating a good accuracy of the proposed colorimetric aptasensor for CAP detection. It was clearly demonstrated that the aptasensor was applicable for the detection of CAP in real milk samples.

4. Conclusion

In summary, a selective, sensitive and facile colorimetric assay was developed for the detection of ultra-trace level of antibiotics, with CAP as model, based on a triple signal amplification strategy with magnetic aptamer-HRP co-immobilized PtNPs nanotracer and Exo I-assisted target recycling. Based on the strong color response, CAP with the concentration as low as 0.01 ng mL^{-1} could be observed with the naked eye, and 0.0003 ng mL^{-1} can be detected by UV-vis spectrum. The proposed method had been successfully applied in real milk samples with a short detection time of 30min. Moreover, the designed assay can be employed to detect other antibiotics when changing the aptamer on the composite probes, which had a promising prospect for in-situ screening toxic antibiotic residues in food and environment.

Acknowledgments

This work was supported by the National Natural Science Foundation of China (Nos. 31070866), the Natural Science Foundation of Zhejiang (LY13C200017), the Natural Science Foundation of Ningbo (2013A610241, 2013A610163, and 2014A610184), the Science and Technology Project of Zhejiang (2013C37033), Non-profit project funded by State Administration of Grain (201313010) and a project funded by the Priority Academic Program Development of Jiangsu Higher Education Institutions (PAPD) and the K.C. Wong Magna Fund in Ningbo University.

References

1 H. E. Carter, D. Gottlieb and H. W. Anderson, Science, 1948, **107**, 113.

2 A. Gantverg, I. Shishani and M. Hoffman, Analytica Chimica Acta, 2003, **483**, 125–135.

3 M. D. Fedorova, I. P. Andreeva, E. S. Vilegzhanina, A. A. Komarov, M. Y. Rubtsova, J. V. Samsonova and A. M. Egorov, Applied biochemistry and microbiology, 2010, **46**, 795–801.

4 H. T. Rønning, K. Einarsen and T. N. Asp, Journal of Chromatography A, 2006, **1118**, 226–233.

5 X, Yu, Y. He, J. Jiang, H. Cui, Analytica Chimica Acta, 2014, **812**, 236–242.

6 C. Zhou, T. Wang, J. Liu, C. Guo, Y. Peng, J. Bai, M. Liu, J. Dong, Na Gao, B. Ning and Z. Gao, Analyst, 2012, **137**, 4469-4474.

7 X. Tao, H. Jiang, J. Zhu, X. Wang, Z. Wang, L. Niu, X. Wu, W. Shi, J. Shen, Food and Agricultural Immunology, 2014, **25**, 137-148.

8 S. Brox, A. P. Ritter, E. Küster, T. Reemtsma, Analytical and Bioanalytical Chemistry, 2014, **406**, 4831-4840.

9 X. Y. Huang, X. W. Fang, X. Zhang, X. M. Dai & X. L. Guo, H. W. Chen, L. P. Luo, Analytical and bioanalytical chemistry, 2014, **406,** 7705–7714.

10 G. Fedorova, V. Nebesky, T. Randak, R. Grabic, Chemical Papers, 2014, **68**, 29-36.

11 M. Sun, B. Ding, J. Lin, J. Yu, G. Sun, Sensors and Actuators B: Chemical, 2011, **160**, 428-434.

12 M. Ramos, P. Munoz, A. Aranda, I. Rodriguez, R. Diaz, J. Blanca, Journal of

chromatography B, 2003, **791**, 31-38.

13 N. Liu, S. Song, L. Lu, D. Nie, Z. Han, X. Yang, Z. Zhao, A. Wu, X. Zheng, Food and Agricultural Immunology, 2014, **25**, 523-534.

14 J Lee, CH Jeon, SJ Ahn, TH Ha, Analyst, 2014, **139**, 1622-1627.

15 C. C. Huang, Y. F. Huang, Z. Cao, W. Tan and H. T. Chang, Analytical Chemistry, 2005, **77,** 5735–5741.

16 H. Shi, D. Li, F. Xu, X. He, K. Wang, X. Ye, J. Tang, C. He, Analyst, 2014, **139**, 4181-4184.

17 J A .Latham, R. Johnson, JJ. Toole, Nucleic acids research, 1994, **22**, 2817-2822.

18 L C. Bock, L C. Griffin, J A. Latham, E H. Vermaas, J J. Toole, Nature , 1992, **355**, 564−566.

19 C. Tuerk, C. Gold, Science, 1990, **249** 505−510.

20 J. H. Park, Y. S. Cho, S. Kang, E. J. Lee, G. H. Lee, S. S. Hah, Analytical Biochemistry, 2014, **462**, 10–12.

21 Z. Chen, Y. Tan, C. Zhang, L. Yin, H. Ma, N. Ye, H. Qiang, Y. Lin, Biosensors and Bioelectronics, 2014, **56**, 46–50.

22 A. Csordas, A. E. Gerdon, J. D. Adams, J. Qian, S. S. Oh, Y. Xiao and H. T. Soh, Angewandte Chemie International Edition, 2010, **49**, 355–358.

23 W. Emlen, R. Ansari, and G. Burdick, the Journal of Clinical Investigation, 1984, **74**, 185-190.

24 G. Burdick and W. Emlen, the Journal of Immunolcgy, 1985, **135**, 2593-2597.

25 A. Morrin, A. Guzmanb, A. J. Killarda, J. M. Pingarronb, M. R. Smyth, Biosensors

and Bioelectronics, 2003, **18**, 715–720.

26 A. Frey, B. Meckelein, D. Externest, M. A. Schmidt, Journal of Immunological Methods, 2000, **233**, 47–56.

27 E. S. Bos, A. A. van der Doelen, N. van Rooy & A. H.W.M., Journal of Immunoassay, 1981, **2**, 187-204.

28 I. Willner, B. Basnar and B. Willner, Febs Journal, 2007, **274**, 302–309.

29 Z. Gao, L. Hou, M. Xu and D. Tang, Scientific reports, 2014, **10**, 3966

30 R. Sharma, D. N. Rao, Journal of Molecular Biology, 2009, **385**, 1375–1396

31 W. Wen, R. Hu, T. Bao, X. Zhang, S. Wang, Biosensors and Bioelectronics, 2015, **71**, 13–17.

32 X. Yan, M. Sperling, and B. Welz, Analytical Chemistry, 1999, **71**, 4353–4360.

33 J. Wang, L. Yang, S. Boriskina, B. Yan, and B. M. Reinhard, Analytical Chemistry, 2011, **83**, 2243–2249.

34 J. Mehta, B. Van Dorst, E. Rouah-Martin, W. Herrebout, M. Scippo,R. Blust, J. Robbens, Journal of Biotechnology, 2011, **155**, 361–369.

35 H. Deng, X. Li, Q. Peng, X. Wang, J. Chen, Y. Li, Angewandte Chemie International Edition, 2005, **117**, 2842-2845.

36 G. Frens, Nature, 1972, **241**, 20-22.

37 X. Chen, J. Zhu, Z. Chen, C. Xu, Y. Wang, C. Yao, Sensors and Actuators B: Chemical 2011, **159**, 220-228.

38 S. Xu, H. Yuan, A. Xu, J. Wang, L. Wu, Journal of the American Chemical Society 2011, **27**, 13629–13634.

39 G M Wahl, M Stern, and G R Stark, Proceedings of the National Academy of Sciences Of the United States of America, 1979, **76**, 3683–3687.

40 H. Zhang, J. Xu, and H. Chen, Analytical Chemistry, 2013, **85**, 5321–5325.

41 S. Wang, R. Hu, W. Wen, Q. Wang, H. Xiong, X. Zhang, H. Gu, Biosensors and Bioelectronics, 2014, 53, 384–389.

42 N. Gan, X. Du, Y. Cao, Hu, T. Li and Q. Jiang, An Materials, 2013, **6**, 1255-1269.

43 X. Que, D. Tang, B. Xia, M. Lu, D. Tang, Analytica Chimica Acta, 2014, **830**, 42-48.

44 G. Yang, F. Zhao, Biosens. Bioelectron, 2015, **64**, 416-422.

45 S. Wu, H. Zhang, Z. Shi, N. Duan, C. Fang, S. Dai, Z. Wang, Food Control, 2015, **50**, 597-604.

46 K. Kor, K.Zarei, Journal of Electroanalytical Chemistry, 2014, **733**, 39-46.

47 X. Yu, Y. He, J. Jiang, H. Cui, Analytica Chimica Acta, 2014, **812**, 236-242.

48 Y. Lu, Q. Shen, Z. Dai, H. Zhang, Analytical and Bioanalytical Chemistry, 2010, **398,** 1819-1826.

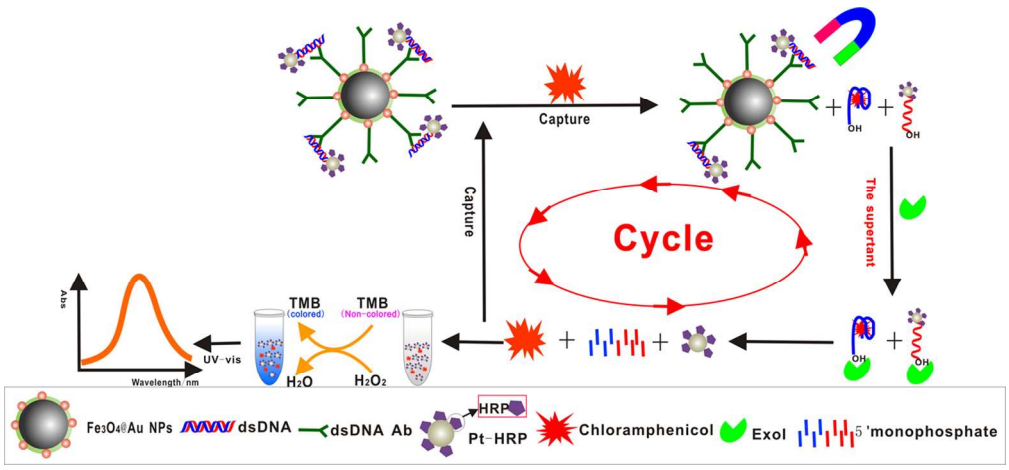

Scheme 1 The detection procedures and color development for CAP

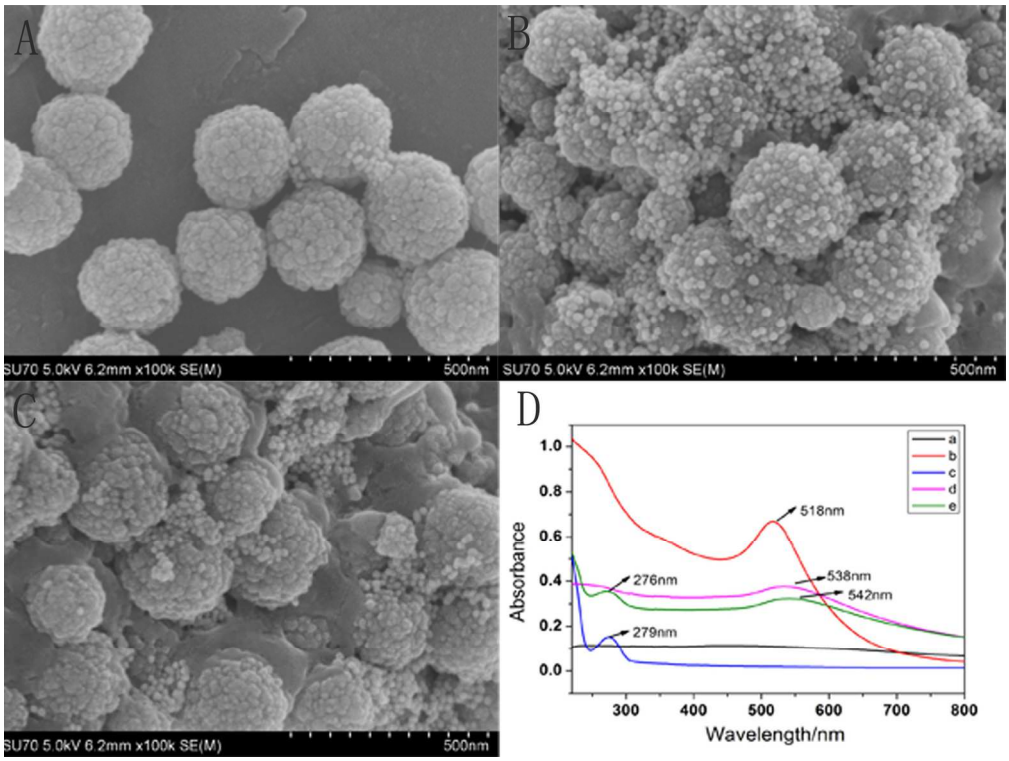

Fig. 1 SEM images of (A) bare Fe3O4NPs, (B) AuMNPs, (C) dsDNA Ab-AuMNPs, (D) UV-vis spectra of Fe3O4NPs (a), AuNPs (b), dsDNA Ab (c), AuMNPs (d), AuMNPs-dsDNA Ab conjugates (e).
142x107mm (300 x 300 DPI)

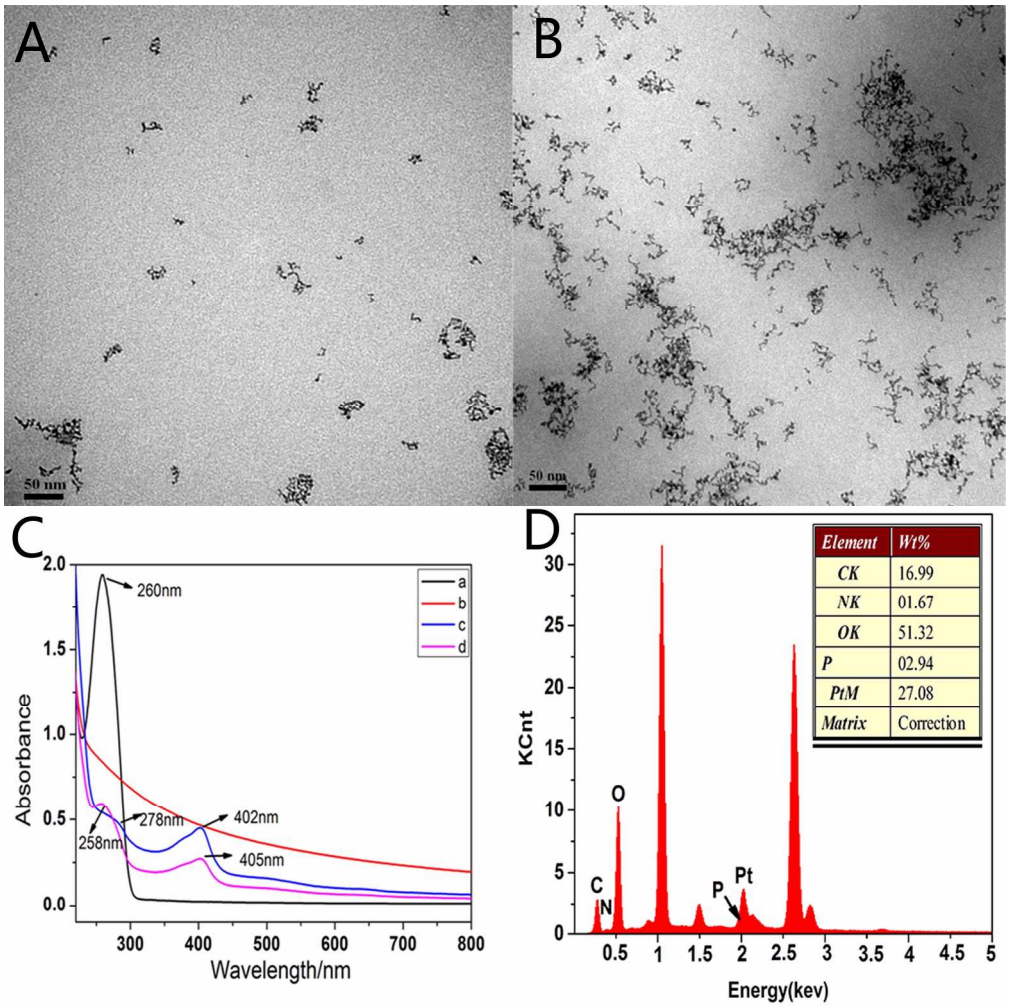

Fig. 2 (A)TEM images of Pt NPs, (B) HRP-PtNPs (C) UV-vis spectra of ds-Apt (a), Pt NPs (b), HRP (c) and ds-Apt-Pt NPs-HRP (d), and (D) the energy-dispersive X-ray spectroscopy of ds-Apt-HRP-PtNPs.
211x211mm (300 x 300 DPI)

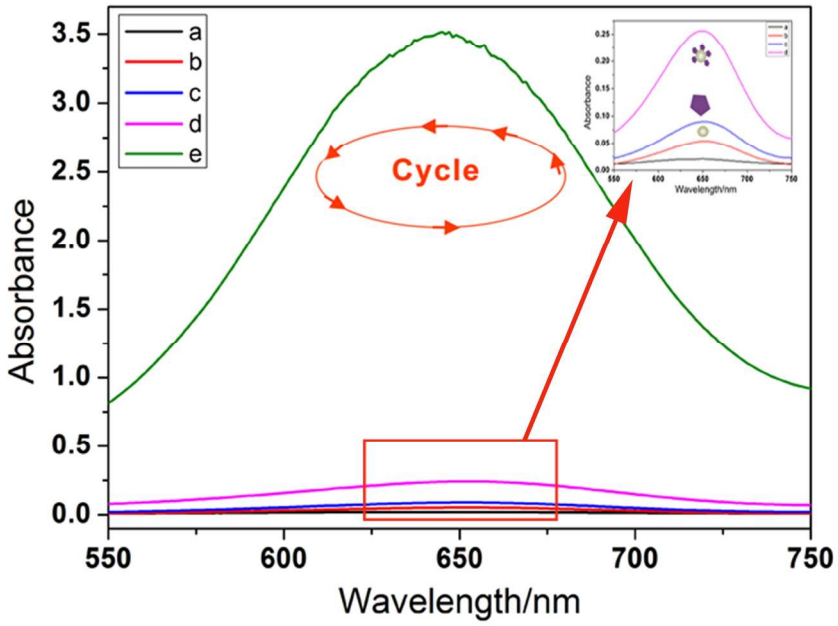

Fig. 3 The colorimetric responses of the aptasensor before adding CAP in 0.85 μM TMB- 0.45 μM H2O2 (a) and after adding 100 ng mL-1 CAP and incubation for 30 min with PtNPs as signal probe (b), dsApt-HRP as signal probe (c) or PtNPs-HRP nanotracer as signal probe (d), and PtNPs- HRP with 20U Exo I (e). All the experiments were processed with incubating at 37 °C the 0.1 M PBS.
200x139mm (300 x 300 DPI)

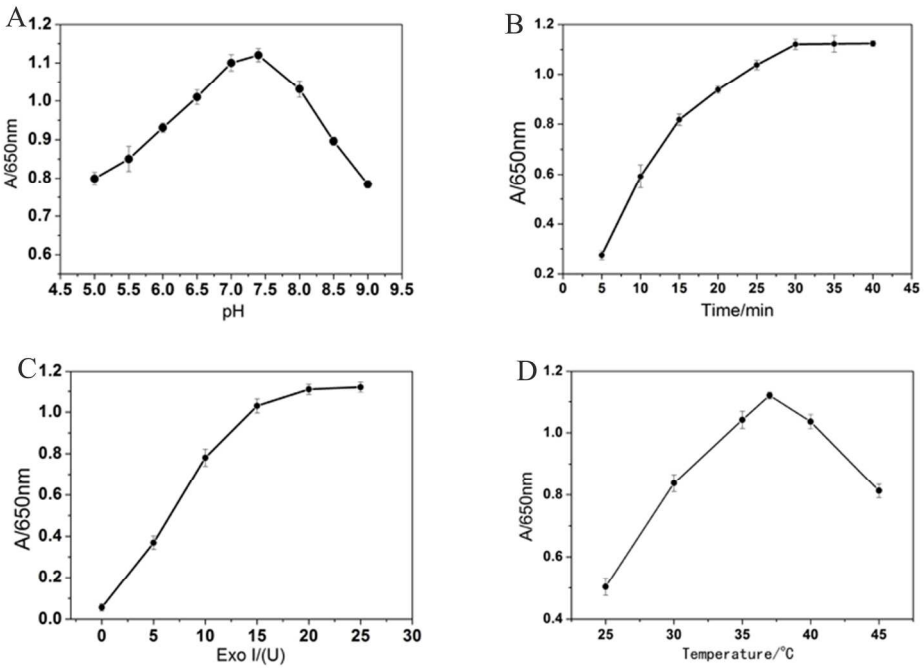

Fig. 4 (A) UV-vis absorption spectra of the proposed colorimetric aptasensor in the presence of different pH of detection solution (5, 5.5, 6, 6.5, 7, 7.5, 8, 8.5, 9), (B) incubation time from 5 to 45 min, (C) The Exo I concentration was optimized in the Exo I (from down to up: 0, 5, 10, 15, 20 and 25 U), (D) incubation temperature from 25 °C to 40 °C, All the experiments were processed with the 0.1 M pH 7.4 PBS containing 10 ng mL-1 of CAP
205x142mm (300 x 300 DPI)

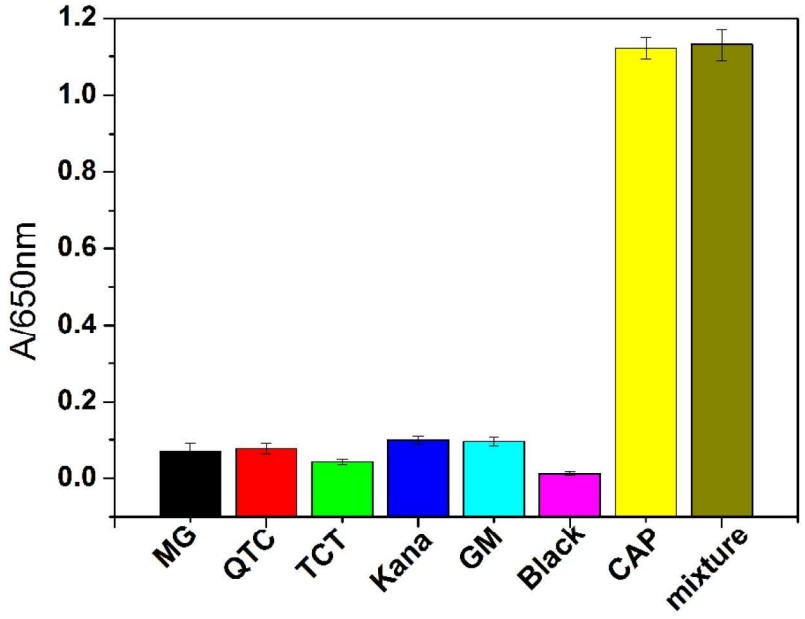

Fig. 5 The selectivity test of the developed colorimetric aptasensor.
200x139mm (300 x 300 DPI)

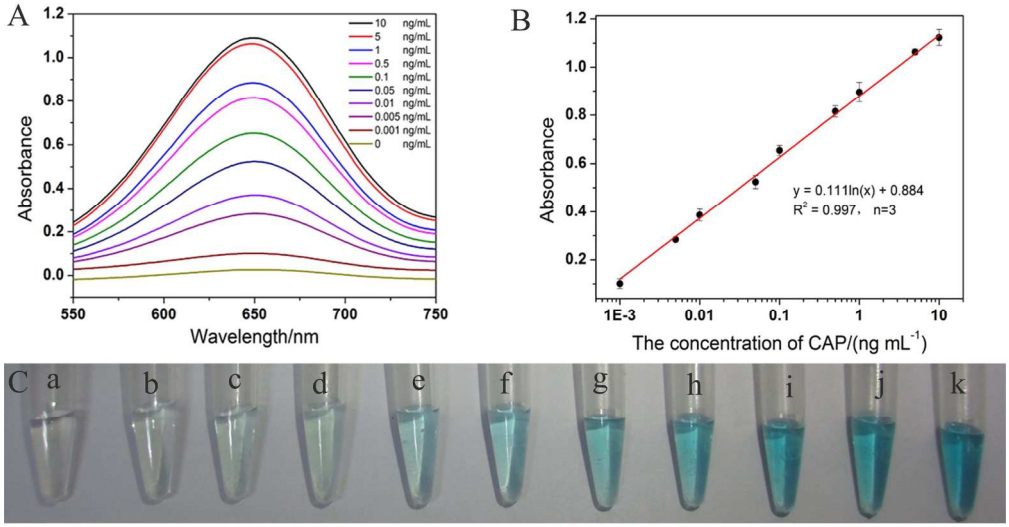

Fig. 6 UV-vis absorption spectra of the proposed colorimetric aptasensor in the presence of different concentrations of CAP target, (B) calibration plot of the proposed colorimetric aptasensor in the presence of different concentrations of CAP target. And C shows the corresponding digital camera pictures of colorimetric responses of different amounts of target CAP. The concentration of CAP are 0, 0.01, 0.02, 0.05, 0.1, 0.2, 0.5, 1, 2, 5, 10ng mL-1, respectively.
175x93mm (300 x 300 DPI)

Table. 1 The current detection methods for CAP, the linear range, the limit of detection (LOD) and the reaction time with target

Method	Target analyte: CAP ($ng\ mL^{-1}$)		Reaction time with target (min)	Reference
	Linear range	limit of detection (LOD)		
Gold nanocatalyst-based immunosensing	0.1-100	0.03	-	43
MWCNTs@MIP electrochemical sensor	1.625-1292.5	0.0325	-	44
Fluorescence biosensor	0.01-1	0.01	60	45
Electrochemical aptasensor	0.52-135.6	0.52	60	46
competitive immunoassay	10-1000	7.6	60	47
HPLC-MS/MS immunoassay	0.1-100	0.04	120	48
Colorimetric aptasensor	0.001-10	0.0003	30	This work

Note: The symbol '- 'suggest that the result could not be clearly stated in the article.

Table 2. The developed method and ELISA method for CAP detection ($\bar{x}$±s, n=5).

Samples number	Blank (ng mL^{-1})	Added (ng mL^{-1})	Proposed method (ng mL^{-1})	ELISA (ng mL^{-1})	Recovery (%)
1	0.12	0.10	0.21±0.01	-	90.0
	0.12	1.00	1.10±0.02	1.03±0.04	98.0
2	0	0.10	0.09±0.01	0.08±0.01	90.0
	0	1.00	1.08±0.08	1.02±0.12	100.8
3	0	0.10	0.09±0.02	0.07±0.03	90.0
	0	1.00	1.02±0.11	1.22±0.24	102.0

Note: The symbol '- 'suggest that the sample could not be detected by the corresponding method.